# Adjustment of ocean color sensor calibration through multi-band statistics

**Richard P. Stumpf [1*] and P. Jeremy Werdell [2]**

[1]*NOAA National Ocean Service, 1305 East–west Highway N/SCI1, Silver Spring, Maryland 20910, USA*
[2]*Science Systems and Applications, Inc., NASA Goddard Space Flight Center, Greenbelt, Maryland 20771, USA*
** richard.stumpf@noaa.gov*

**Abstract**: The band-by-band vicarious calibration of on-orbit satellite ocean color instruments, such as SeaWiFS and MODIS, using ground-based measurements has significant residual uncertainties. This paper applies spectral shape and population statistics to tune the calibration of the blue bands against each other to allow examination of the interband calibration and potentially provide an analysis of calibration trends. This adjustment does not require simultaneous matches of ground and satellite observations. The method demonstrates the spectral stability of the SeaWiFS calibration and identifies a drift in the MODIS instrument onboard Aqua that falls within its current calibration uncertainties.



**OCIS codes:** (010.0010) Atmospheric and oceanic optics; (010.1285) Atmospheric correction; (120.5630) Radiometry; (280.0280) Remote sensing and sensors.

## References and links

1. J. E. O'Reilly, S. Maritorena, B. G. Mitchell, D. A. Siegel, K. L. Carder, S. A. Garver, M. Kahru, and C. McClain, "Ocean color chlorophyll algorithms for SeaWiFS," J. Geophys. Res. **103**(C11), 24937–24953 (1998).
2. S. Maritorena, D. A. Siegel, and A. R. Peterson, "Optimization of a semianalytical ocean color model for global-scale applications," Appl. Opt. **41**(15), 2705–2714 (2002).
3. Z. Lee, K. L. Carder, and R. A. Arnone, "Deriving inherent optical properties from water color: a multiband quasi-analytical algorithm for optically deep waters," Appl. Opt. **41**(27), 5755–5772 (2002).
4. B. A. Franz, E. J. Kwiatkowska, G. Meister, and C. R. McClain, "Moderate Resolution Imaging Spectroradiometer on Terra: limitations for ocean color applications," J. Appl. Remote Sens. **2**(1), 023525 (2008), doi:10.1117/1.2957964.
5. P. J. Werdell, S. W. Bailey, B. A. Franz, A. Morel, and C. R. McClain, "On-orbit vicarious calibration of ocean color sensors using an ocean surface reflectance model," Appl. Opt. **46**(23), 5649–5666 (2007).
6. R. E. Eplee, Jr., R. A. Barnes, F. S. Patt, G. Meister, and C. R. McClain, "SeaWiFS lunar calibration methodology after six years in orbit," Proc. SPIE **5524**, (2004), doi:10.1117/12.556408.
7. B. A. Franz, S. W. Bailey, P. J. Werdell, and C. R. McClain, "Sensor-independent approach to the vicarious calibration of satellite ocean color radiometry," Appl. Opt. **46**(22), 5068–5082 (2007).
8. D. K. Clark, H. R. Gordon, K. J. Voss, Y. Ge, W. Broenkow, and C. Trees, W.W. Broenkow, and C. Trees, "Validation of atmospheric correction over the oceans," J. Geophys. Res. **102**(D14), 17209–17217 (1997).
9. IOCCG, *Ocean-Colour Data Merging*, Reports of the International Ocean-Colour Coordinating Group, No. 6 (IOCCG, 2007).
10. R. Letelier, and M. R. Abbott, "An analysis of chlorophyll fluorescence algorithms for the Moderate Resolution Imaging Spectrometer (MODIS)," Remote Sens. Environ. **58**(2), 215–223 (1996).
11. J. F. R. Gower, R. Doerffer, and G. A. Borstad, "Interpretation of the 685 nm peak in water-leaving radiance spectra in terms of fluorescence, absorption, and scattering and its observation by MERIS," Int. J. Remote Sens. **20**, 1771–1786 (1999).
12. J. F. R. Gower, S. King, G. Borstad, and L. Brown, "Detection of intense plankton blooms using the 709 nm band of the MERIS imaging spectrometer," Int. J. Remote Sens. **26**(9), 2005–2012 (2005).
13. S. Alvain, C. Moulin, Y. Dandonneau, and F. M. Breon, "Remote sensing of phytoplankton groups in case 1 waters from global SeaWiFS imagery," Deep Sea Res. Part I Oceanogr. Res. Pap. **52**(11), 1989–2004 (2005).
14. A. Subramaniam, R. R. Hood, C. W. Brown, E. J. Carpenter, and D. G. Capone, "Detecting Trichodesmium blooms in SeaWiFS imagery," Deep Sea Res. Part II Top. Stud. Oceanogr. **49**(1-3), 107–121 (2001).
15. T. T. Wynne, R. P. Stumpf, M. C. Tomlinson, R. A. Warner, P. A. Tester, J. Dyble, and G. L. Fahnenstiel, "Relating spectral shape to cyanobacterial blooms in the Laurentian Great Lakes," Int. J. Remote Sens. **29**(12), 3665–3672 (2008).

#114396 - $15.00 USD Received 16 Jul 2009; revised 13 Nov 2009; accepted 1 Dec 2009; published 4 Jan 2010

16. M. C. Tomlinson, T. T. Wynne, and R. P. Stumpf, "An evaluation of remote sensing techniques for enhanced detection of the toxic dinoflagellate, Karenia brevis," Remote Sens. Environ. **113**(3), 598–609 (2009).
17. P. Shanmugam, and Y. H. Ahn, "New atmospheric correction technique to retrieve the ocean colour from SeaWiFS imagery in complex coastal waters," J. Opt. Soc. Am. A **9**, 511–530 (2007).
18. NASA Ocean Biology Processing Group, "Ocean Color Reprocessing 2009," http://oceancolor.gsfc.nasa.gov/REPROCESSING/R2009/ (2009).
19. R. A. Schowengerdt, *Remote Sensing, Models and Methods for Image Processing* (Academic, 1997).
20. C. R. McClain, S. B. Hooker, G. C. Feldman, and P. Bontempi, "Satellite data for ocean biology, biogeochemistry, and climate research," Eos Trans. AGU **87**(34), 337 (2006).
21. B. A. Franz, P. J. Werdell, G. Meister, S. W. Bailey, R. E. Eplee, Jr., G. C. Feldman, E. Kwiatkowska, C. R. McClain, F. S. Patt, and D. Thomas, "The continuity of ocean color measurements from SeaWiFS to MODIS," Proc. SPIE **5882**, (2005), doi:10.1117/12.620069.
22. H. R. Gordon, and M. Wang, "Retrieval of water-leaving radiance and aerosol optical thickness over the oceans with SeaWiFS: a preliminary algorithm," Appl. Opt. **33**(3), 443–452 (1994).
23. R. P. Stumpf, R. A. Arnone, R. W. Gould, Jr., P. Martinolich, and V. Ransibrahmanakul, "Partially coupled ocean-atmosphere model for retrieval of water-leaving radiance from SeaWiFS in coastal waters," in *Algorithm Updates for the Fourth SeaWiFS Data Reprocessing*, NASA Tech. Memo. 206892 Vol. 22. S.B. Hooker and E. R. Firestone, eds. (NASA Goddard Space Flight Center, 2003) pp. 51–59.
24. A. Morel, D. Antoine, and B. Gentili, "Bidirectional reflectance of oceanic waters: accounting for Raman emission and varying particle scattering phase function," Appl. Opt. **41**(30), 6289–6306 (2002).
25. F. S. Patt, R. A. Barnes, R. E. Eplee, Jr., B. A. Franz, W. D. Robinson, G. C. Feldman, S. W. Bailey, J. Gales, P. J. Werdell, M. Wang, R. Frouin, R. P. Stumpf, R. A. Arnone, R. W. Gould, Jr., P. M. Martinolich, V. Ransibrahmanakul, J. E. O'Reilly, and J. A. Yoder, *Algorithm Updates for the Fourth SeaWiFS Data Reprocessing*, NASA Tech. Memo. 206892 Vol. 22 (NASA Goddard Space Flight Center, 2002).
26. P. J. Werdell, S. W. Bailey, B. A. Franz, L. W. Harding, Jr., G. C. Feldman, and C. R. McClain, "Regional and seasonal variability of chlorophyll-a in Chesapeake Bay as observed by SeaWiFS and MODIS-Aqua," Remote Sens. Environ. **113**(6), 1319–1330 (2009).
27. E. J. Kwiatkowska, B. A. Franz, G. Meister, C. R. McClain, and X. Xiong, "Cross calibration of ocean-color bands from moderate resolution imaging spectroradiometer on Terra platform," Appl. Opt. **47**(36), 6796–6810 (2008).
28. D. Jolivet, D. Ramon, P.-Y. Deschamps, F. Steinmetz, B. Fougnie, and P. Henry, "How the ocean color product quality is limited by atmospheric correction," Proc. Envisat Symposium 2007, Montreux, Switzerland (2007).

## 1. Introduction

Satellite sensors that make quantitative ocean color radiometric measurements require a more exacting calibration than do land sensors because of the small signal of the ocean relative to the atmosphere. As several spectral bands are involved in bio-optical algorithms used to estimate geophysical data products from these radiances [1–3], absolute calibration errors can be magnified. With 90% or more of the signal at the satellite coming from the atmosphere, a 0.5% spectral calibration error under the best conditions will result in errors of 5% or greater in derived spectral normalized water–leaving radiances ($nL_w(\lambda)$; units of μW cm$^{-2}$ nm$^{-1}$ sr$^{-1}$), and these errors propagate into the secondary bio-optical algorithms [4,5]. Maintaining accurate and consistent inter-band calibration will assure meaningful analysis of data and of temporal trends in imagery.

The on-orbit calibration of ocean color sensors, in particular, the National Aeronautics and Space Administration (NASA) Sea-viewing Wide-Field-of-View Sensor (SeaWiFS) and the NASA Moderate Resolution Imaging Spectroradiometer (MODIS), depends on a combination of techniques, the general flow of which is described as follows. First, absolute spectral calibrations are made pre-launch. After launch, additional adjustments for time dependence in each spectral band are made using the Sun or the moon as a reference [6], provided the sensor can point at the moon. Finally, the absolute calibration is adjusted on-orbit using a reference to spectral earth surface measurements, a method termed "vicarious calibration" [7].

The vicarious calibration uses temporally and spatially coincident "match-ups" with ground reference data to adjust the pre-launch calibration. For SeaWiFS and MODIS, the reference is the Marine Optical Buoy (MOBY) [8]. This approach inherently corrects the combination of instrument plus atmospheric correction by adjusting the instrument calibration to the standard aerosol models and algorithms used to remove atmospheric interference from the data. Each band is calibrated independently, with an uncertainity of 0.8% [7]. As a result

#114396 - $15.00 USD Received 16 Jul 2009; revised 13 Nov 2009; accepted 1 Dec 2009; published 4 Jan 2010

of this uncertainty and the relatively few matchups that can be made each year, this calibration is insufficient to address instrument drift [7]. The lunar reference provides the relative precision needed for adjusting instrument drift, with radiometric stability at the top-of-the-atmosphere better than 0.07% over the mission [6]. It does not achieve the absolute accuracy required to adjust the absolute calibration. Unfortunately, not all sensors or satellites observe the moon owing to the need for sophisticated changes in satellite orientation; for example, SeaWiFS makes monthly observations whereas MODIS does so less frequently.

With several ocean color instruments currently in orbit and others proposed for development, calibration accuracy becomes critical for assuring meaningful inter-comparison amongst the sensors [9]. On-orbit calibration might be enhanced using techniques that provide independent information on temporal patterns and the relative calibration of the bands. For example, Werdell and co-authors [5] proposed using water-leaving radiances derived from a spectral ocean surface reflectance model as ground reference data for the vicarious calibration of sensors with a paucity of coincident in situ radiometric measurements. The difficulty remains in establishing an ability to refine such techniques or to address temporal trends in the data in the absence of a rigorous temporal (e.g., lunar) calibration. Because the current vicarious methods for absolute calibration depend on coincident "match-ups" (same day and time) of a reference site (e.g., MOBY) and satellite measurements, methods with relaxed requirements on coincidence (a process that limits the statistical sample size) could aid in improving calibrations.

Analysis of spectral shape offers a tool to examine the relative characteristics of several bands. Derivatives are a common example of spectral shapes and are less dependent on calibration than are ratios. The first derivative, or slope, provides information on two bands; the second derivative, a curvature measure, examines three bands simultaneously. Recently, spectral shapes have been used as algorithms to detect optical features. These include several methods that are numerically equivalent to the second derivative: fluorescence line height [10]; Modified Chlorophyll Index [11,12]; and, several algae identification methods [13–16]. Analysis of spectral shape has also been proposed as a tool for atmospheric correction [17].

Bio-optical algorithms for SeaWiFS and MODIS predominantly use blue spectral bands. The three-band Ocean Color Chlorophyll algorithm (OC3) uses 443 and 490 nm [1]. Algorithms for quantifying chromophoric dissolved organic matter (CDOM) require 412 nm [2,3]. While the current calibration treats each band independently, the relevant interband calibration is a critical part of assuring robust bio-optical algorithms. This paper will examine spectral shape as a method for examining and evaluating on-orbit spectral characteristics and the vicarious calibration of space-borne ocean color instruments, using these blue bands as an example. Recently, MODIS onboard the Aqua platform has shown a drift in its 412 nm band, particularly in 2007 and 2008 [18], which was first identified in global statistics of $nL_w(\lambda)$. We use these data for a preliminary case study to demonstrate how identifying and correcting such patterns using spectral shapes can provide an improvement in calibration.

## 2. Methods

### *2.1 Calculation of spectral shape*

A common method for quantifying spectral shape (*SS*) is via curvature, which allows a comparison of the relative radiance of three adjacent bands. We define SS as a variant of the second derivative:

$$SS(\lambda) = R_{rs}(\lambda) - R_{rs}(\lambda^-) - \left[R_{rs}(\lambda^+) - R_{rs}(\lambda^-)\right]\left(\frac{\lambda - \lambda^-}{\lambda^+ - \lambda^-}\right) \quad (1)$$

where $R_{rs}$ is the remote sensing reflectance (units of $sr^{-1}$; the ratio of water-leaving radiance to downwelling surface irradiance), $\lambda$ is the central wavelength, $\lambda^+$ is the next higher wavelength,

#114396 - $15.00 USD Received 16 Jul 2009; revised 13 Nov 2009; accepted 1 Dec 2009; published 4 Jan 2010

and $\lambda^-$ is the next lower wavelength. If the bands are evenly spaced, such that $(\lambda^+ - \lambda) = (\lambda - \lambda^-)$, Eq. (1) reduces to a form that is equivalent to the numerical second derivative [19]. A positive spectral shape indicates a "hill" (corresponding to a negative second derivative) and a negative spectral shape indicates a "valley" (corresponding to a positive second derivative). Unlike ratios, derivatives are insensitive to magnitudes. For a ratio, $R_{rs}(\lambda^+) / R_{rs}(\lambda)$, a change in gain, $\Delta$ (such that we have $[R_{rs}(\lambda^+) + \Delta] / [R_{rs}(\lambda) + \Delta]$), results in an error of $\Delta / R_{rs}(\lambda)$. In contrast, simple algebra shows that a gain change, $\Delta$, drops out of Eq. (1). A common example of applying spectral shape to ocean optical remote sensing is the calculation of fluorescent line height from three $nL_w(\lambda)$ in the red spectral range [10]. In open ocean waters, $\lambda$ may be between 443 and 510 for SeaWiFS and between 443 and 531 for MODIS (the reflectance at wavelengths longer than 600 nm is too small to be meaningful).

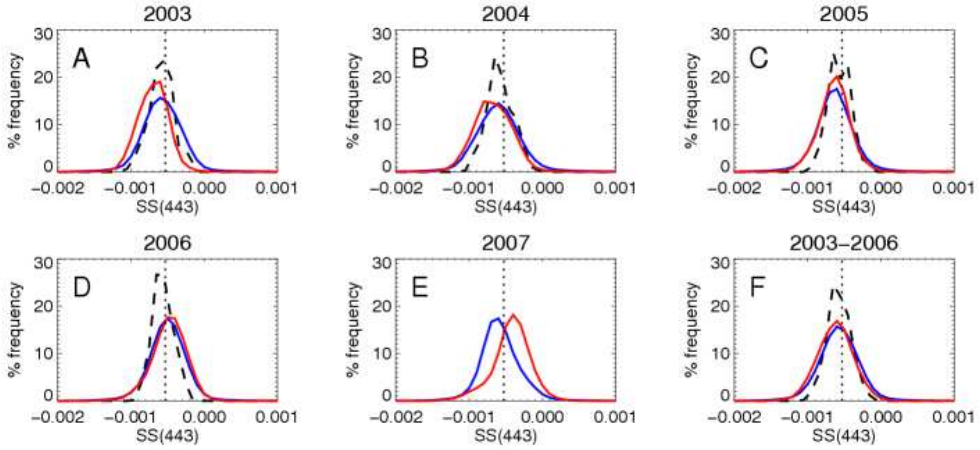


Fig. 1. Annual relative frequency distributions for *SS*(443) for SeaWiFS (blue lines), Aqua (red lines), and MOBY (black dashed). Population histograms of *SS*(443) were generated using a bin size of 0.0001. The median value for the cumulative (2003-2006) MOBY distribution ( = –0.00053) is indicated in each panel by the vertical dotted line.

### *2.2 In situ data*

The MOBY is used as the standard ground reference for the vicarious calibration of SeaWiFS and MODIS. As such, the MOBY is the appropriate ground reference to examine the use of spectral shape statistics for the calibration. MOBY is located approximately 20 miles west of Lanai, Hawaii, and is used for the operational vicarious calibration of SeaWiFS and MODIS [7]. MOBY routinely measures upwelling radiance ($L_u$; units of $\mu W\ cm^{-2}\ nm^{-1}\ sr^{-1}$) at nominal depths of 1, 5, and 9 meters and surface irradiance ($E_s$; units of $\mu W\ cm^{-2}\ nm^{-1}$), all in the spectral range 340-955 nm at 0.6 nm spectral resolution [8]. The $L_u(\lambda,z)$ are extrapolated to the sea surface to estimate $nL_w(\lambda)$, which are subsequently used as ground reference data for the vicarious calibration of the satellite radiometry. For this analysis, hyperspectral $R_{rs}(\lambda)$ were convolved to band averages by calculating the mean $R_{rs}$ from $\lambda_{i\text{-}5nm}$ to $\lambda_{i\,+\,5nm}$, where $\lambda_i$ are the center wavelengths of SeaWiFS and MODIS blue-green bands. All available MOBY observations were used in this analysis. Two or three samples are taken per day, with the number of samples per year ranging from 456 in 2003 to 722 in 2005.

### *2.3 Satellite data*

Extracted SeaWiFS and MODIS on Aqua Level-1A files containing all or part of the region around MOBY were acquired from the NASA Ocean Biology Processing Group (OBPG) [20]. MODIS on Aqua is hereon referred to as Aqua. MODIS on Terra was not examined in this paper. The SeaWiFS and Aqua data sets both provide ~1.1 $km^2$ spatial resolution at nadir

#114396 - $15.00 USD Received 16 Jul 2009; revised 13 Nov 2009; accepted 1 Dec 2009; published 4 Jan 2010

(SeaWiFS data were limited to Merged Local Area Coverage files). We considered a near full-time series for both sensors, namely January 1998 to December 2007 for SeaWiFS and June 2002 to December 2007 for Aqua. The lack of SeaWiFS data from January to August 2008 precluded our extending the time-series to present day. Level-2 files were generated using the OBPG processing software MSl12 [21] largely configured for SeaWiFS Reprocessing 5.2 and Aqua Reprocessing 1.1, which includes the Gordon and Wang [22] atmospheric correction approach, plus corrections for near-infrared $nL_w$, bi-directional reflectance, and spectral band-pass effects [23–25]. All methods for instrument calibration and processing are applied identically to both sensors [7]. The operational pixel-masking scheme for each sensor was adopted and the quality control metrics described in Werdell and co-authors [26] were applied to ensure than only the most reliable data were retained for analysis. For each satellite image, spectral shapes were calculated for each unmasked pixel in a square 0.25° box centered on the nominal position of MOBY (20.8°N, −157.2°W).

**Table 1. Population medians and the RMS error against MOBYof the monthly means for the *SS*(443) frequency distributions presented in Fig. 1.**

| | MOBY | SeaWiFS | Aqua | RMS SeaWiFS-MOBY | RMS Aqua-MOBY |
|---|---|---|---|---|---|
| 2003 | –0.00052 | –0.00051 | –0.00064 | $0.83 \times 10^{-4}$ | $1.23 \times 10^{-4}$ |
| 2004 | –0.00055 | –0.00054 | –0.00062 | $0.81 \times 10^{-4}$ | $1.07 \times 10^{-4}$ |
| 2005 | –0.00052 | –0.00056 | –0.00058 | $1.08 \times 10^{-4}$ | $1.06 \times 10^{-4}$ |
| 2006 | –0.00052 | –0.00044 | –0.00042 | $0.94 \times 10^{-4}$ | $1.20 \times 10^{-4}$ |
| 2007 | | –0.00051 | –0.00037 | | |
| 2003-2006 | –0.00053 | –0.00051 | –0.00056 | $0.89 \times 10^{-4}$ | $1.12 \times 10^{-4}$ |

*2.4 Data analysis*

Two forms of comparison were made. First, all data for single (or multiple) year(s) were accumulated to examine the population distribution through histograms (Fig. 1). The unimodal populations allow for simple comparisons of modes of the different populations. Second, each data set was averaged over a month (following the strategy presented in Werdell and co-authors [26]) and the months were then compared to evaluate temporal patterns (Fig. 2). The data sets from each satellite were compared both to MOBY and to each other.

## 3. Results

The spectral to shape, *SS*(443) for all three sources has a strongly peaked population distribution (Fig. 1). For the time period from 2003 to 2006, SeaWiFS consistently reports the same *SS*(443) population median as MOBY (Table 1). As the sensor was calibrated against MOBY, this match is expected. Aqua shows a different pattern. In 2003, the Aqua median is lower than MOBY (–0.00064 vs. –0.00052). In 2004 and 2005, the two medians are more similar, and in 2006 Aqua has a higher median (although, it appears that SeaWiFS also has a higher median in 2006). Accumulated over the entire time period (2003-2006; Fig. 1F), SeaWiFS, Aqua, and MOBY have similar medians (SeaWiFS: –0.00051, Aqua: –0.00056, MOBY: –0.00053).

#114396 - $15.00 USD Received 16 Jul 2009; revised 13 Nov 2009; accepted 1 Dec 2009; published 4 Jan 2010

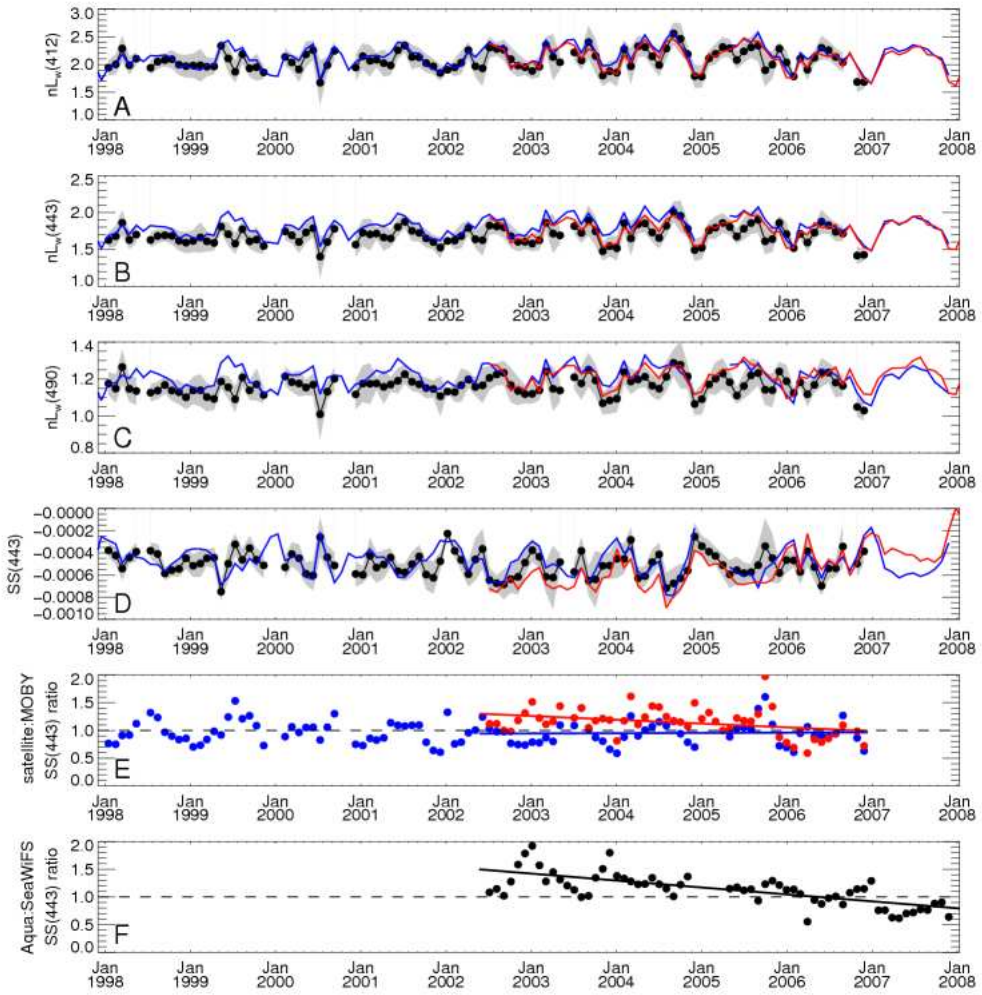


Fig. 2. Monthly time-series for SeaWiFS (blue lines), Aqua (red lines), and MOBY (black circles). Standard deviations for the MOBY averages are shown in gray. Trend lines from Type I linear regression are provided in panels E and F for the Aqua era.

**Table 2. Population medians for the *SS*(443) frequency distributions presented in Fig. 3.**

| | Aqua | | SeaWiFS | |
|---|---|---|---|---|
| | –0.25% | + 0.25% | –0.25% | + 0.25% |
| 2003 | –0.00051 | –0.00077 | –0.00037 | –0.00064 |
| 2004 | –0.00049 | –0.00075 | –0.00040 | –0.00067 |
| 2005 | –0.00045 | –0.00071 | –0.00042 | –0.00070 |
| 2006 | –0.00029 | –0.00055 | –0.00039 | –0.00057 |
| 2007 | –0.00024 | –0.00050 | –0.00037 | –0.00065 |
| 2003-2006 | –0.00043 | –0.00060 | –0.00037 | –0.00064 |

#114396 - $15.00 USD Received 16 Jul 2009; revised 13 Nov 2009; accepted 1 Dec 2009; published 4 Jan 2010

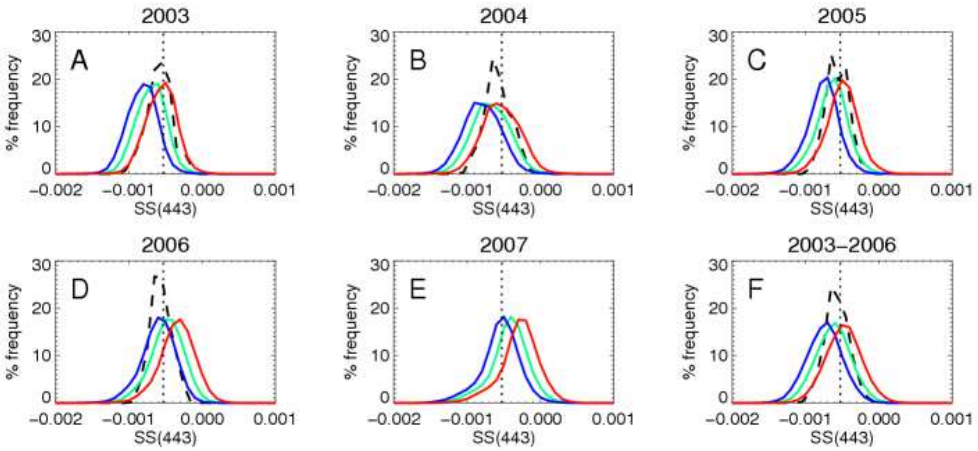


Fig. 3. Annual relative frequency distributions for Aqua and MOBY (black dashed), like Fig. 1. Three Aqua series are shown: standard processing (green) and modified processing with the vicarious gain for 412 nm adjusted by –0.25% (red) and + 0.25% (blue). The median value for the cumulative (2003-2006) MOBY distribution ( = –0.00053) is indicated in each panel by vertical dotted line.

Time series show the difficulty of seeing this pattern in $nL_w(\lambda)$ (Figs. 2A-2C). The $nL_w(\lambda)$ are visually similar for both sensors over their missions, and therefore, trends are not obvious. The monthly mean *SS*(443) shows the trend observed in the annual histograms (Figs. 2D-2F). SeaWiFS shows no long-term trend against MOBY in spectral shape. Aqua, however, shows a change to higher *SS*(443), resulting in a lower ratio against MOBY (as the *SS*(443) is negative). Also, Aqua has a trend against SeaWiFS. Over shorter time scales, the three instruments show seasonal variations in *SS*(443). These correspond to seasonal changes in chlorophyll, although the magnitude of the seasonal shape differs somewhat between MOBY and the satellites.

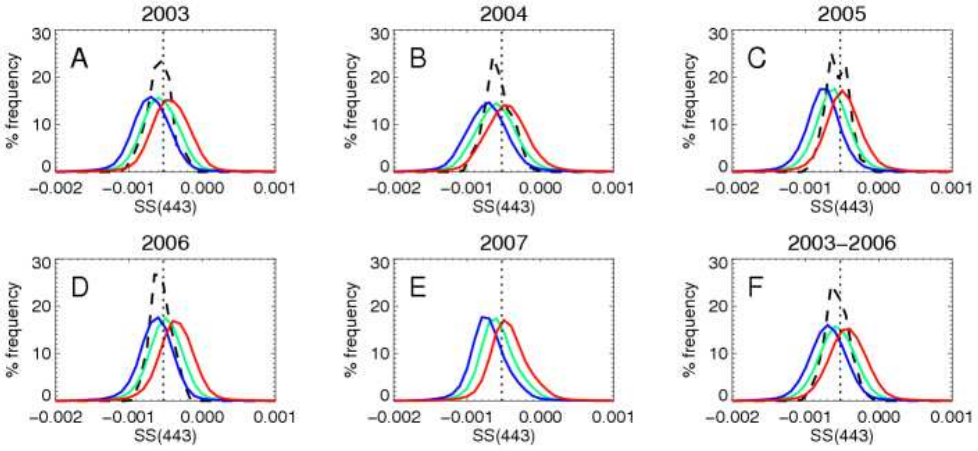


Fig. 4. Annual relative frequency distributions for SeaWiFS and MOBY. See Fig. 3 caption.

## 4. Discussion

### *4.1 Sensitivity*

The cumulative (2003-2006) MOBY *SS*(443) population has a standard deviation (*s*) of 0.00016. The Aqua *SS*(443) medians in 2003 and 2007 fall nearly one standard deviation from

#114396 - $15.00 USD Received 16 Jul 2009; revised 13 Nov 2009; accepted 1 Dec 2009; published 4 Jan 2010

the MOBY cumulative means, namely Aqua at –0.00064 and –0.00037 versus MOBY means (–0.00053) ± *s* of –0.00069 and –0.00037. The difference between the Aqua and MOBY cumulative meanss is statistically significant in an unpaired t-test at $p = 0.01$, with 2003 and 2006 statistically different at $p < 0.0001$. For reference, differences between MOBY and satellite means that exceed $0.2 \times 10^{-4}$ can be statistically different at the 0.05 level (this difference occurred with SeaWiFS in opposite directions in 2005 and 2006). The root mean square (RMS) error between the monthly means from 1998 to 2006 for MOBY and SeaWiFS is $0.9 \times 10^{-5}$. While differences in the monthly data are frequently equal in magnitude to the RMS error (Fig. 2), the annual medians are not (Table 1). This indicates that there may be a limit on the application of this method at a monthly resolution.

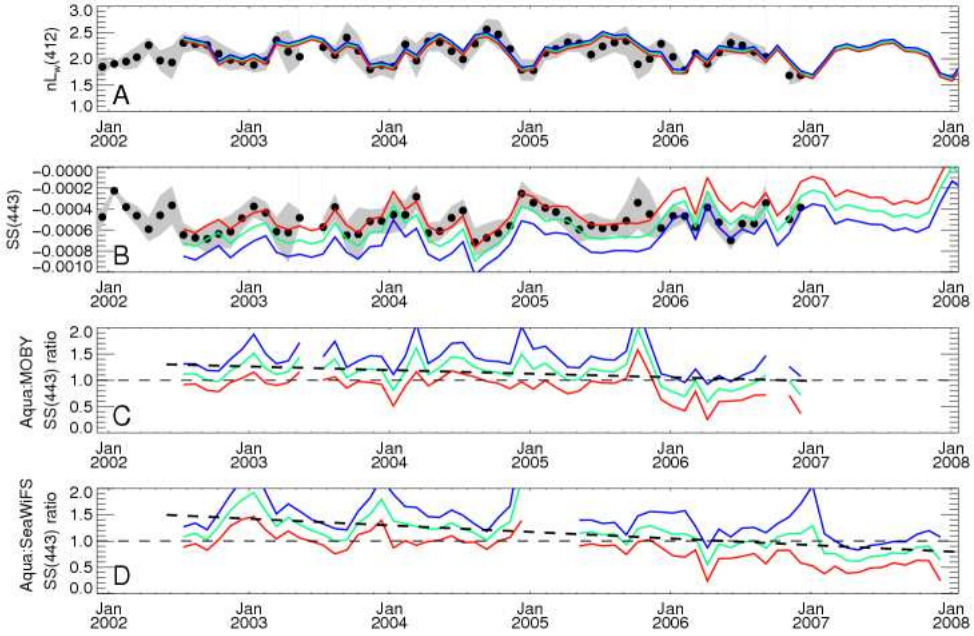


Fig. 5. Monthly time-series for Aqua and MOBY (black circles). Standard deviations for the MOBY monthly averages are shown in gray. Three Aqua series are shown: standard processing (green), modified processing with vicarious gain for 412-nm change by –0.25% (red), and + 0.25% (blue). Trend lines for the standard processing secenario (dashed) from Type I linear regression are provided in panels C and D.

### *4.2 Calibration adjustment*

Our analysis identifies a trend in shape in *SS*(443) for Aqua, indicating a relative temporal shift between the blue bands. For the sole purpose of this case study, we hypothesize that the potential error is a drift in the 412 radiance. A subsequent series of tests identified the degree of calibration change that could introduce the misfit between Aqua and the other instruments. We examined two adjustments from the standard gain: adjusting the gain by ± 0.25%, which corresponds to a gain multiplier of 1.0025 or 0.9975. This adjustment corresponds to a shift of about one standard deviation from the mean in the MOBY data. These adjustments are well within the sensitivity of the original vicarious calibration gain adjustments of 0.8% [7].

The annual frequency histograms (Fig. 3, Table 2) show that these differences can explain the discrepancies in the *SS*(443). In 2003 and 2004, a –0.25% adjustment aligns the Aqua population median with MOBY. In 2005, the standard gain (0% adjustment) matches Aqua with MOBY. In 2006 a + 0.25% adjustment matches Aqua with MOBY. The same analysis

#114396 - $15.00 USD Received 16 Jul 2009; revised 13 Nov 2009; accepted 1 Dec 2009; published 4 Jan 2010

for SeaWiFS suggests that the standard gain best matches MOBY for the full time period (Fig. 4), although the 2006 results show a slight offset.

The time series for Aqua (Fig. 5) gives a representation of the trend. From 2002 until early 2005, a –0.25% adjustment appears to best match the mean MOBY data. In 2005, the standard gain best matches MOBY. By 2006, a + 0.25% adjustment best corresponds with MOBY. In 2007, a + 0.25% adjustment also matches Aqua with SeaWiFS, which continues the relationship observed with MOBY in 2006.

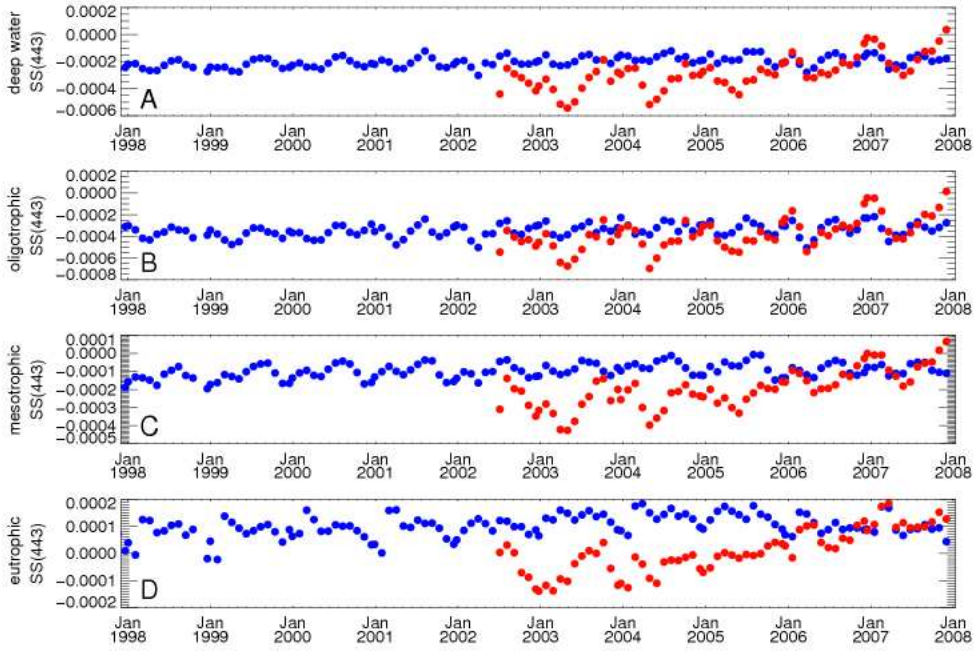


Fig. 6. Monthly time-series for SeaWiFS (blue) and Aqua (red) for four different geographic classifications as defined in the text.

*4.3 Global validation*

To independently verify the results, *SS*(443) were examined from monthly statistics for SeaWiFS and Aqua for the global ocean (Fig. 6). Global, Level-3 composites of $R_{rs}$ were acquired from the OBPG. The spatial and temporal resolutions of the composites were 9 by 9 km equal area bins and 4 days, respectively [21]. To minimize data storage requirements and maximize computational efficiency, only one composite per month was considered (i.e., 4 weeks separate each composite. In the interest of evaluating temporal trends for distinct bioregimes, the data were stratified into a deep water class (water depth > 1000 meters) and three trophic levels: oligotrophic water has satellite chlorophyll less than 0.1 μg $L^{-1}$, mesotrophic water has chlorophyll between 0.1 μg $L^{-1}$and 1.0 μg $L^{-1}$, and eutrophic water has chlorophyll greater than 1.0 μg $L^{-1}$. To facilitate the use of common geographic areas for both sensors in this stratification, the mission-long SeaWiFS chlorophyll composite (September 1997 to 2008) was used to define, a priori, the spatial boundaries of each trophic regime. Those bins with valid pixels for both sensors were identified and averaged to create time-series trends of *SS*(443). In this case we looked only for trends. SeaWiFS was stable over the time period in all water types. Aqua showed the same trend in all water types. In eutrophic water, the spectral shape is positive for SeaWiFS, i.e., *SS*(443) > 0. Aqua, however, started with a negative spectral shape in eutrophic water and did not reach a positive shape until 2006, which indicates a fundamental shift in the relationship of its blue (412-490) bands.

#114396 - $15.00 USD Received 16 Jul 2009; revised 13 Nov 2009; accepted 1 Dec 2009; published 4 Jan 2010

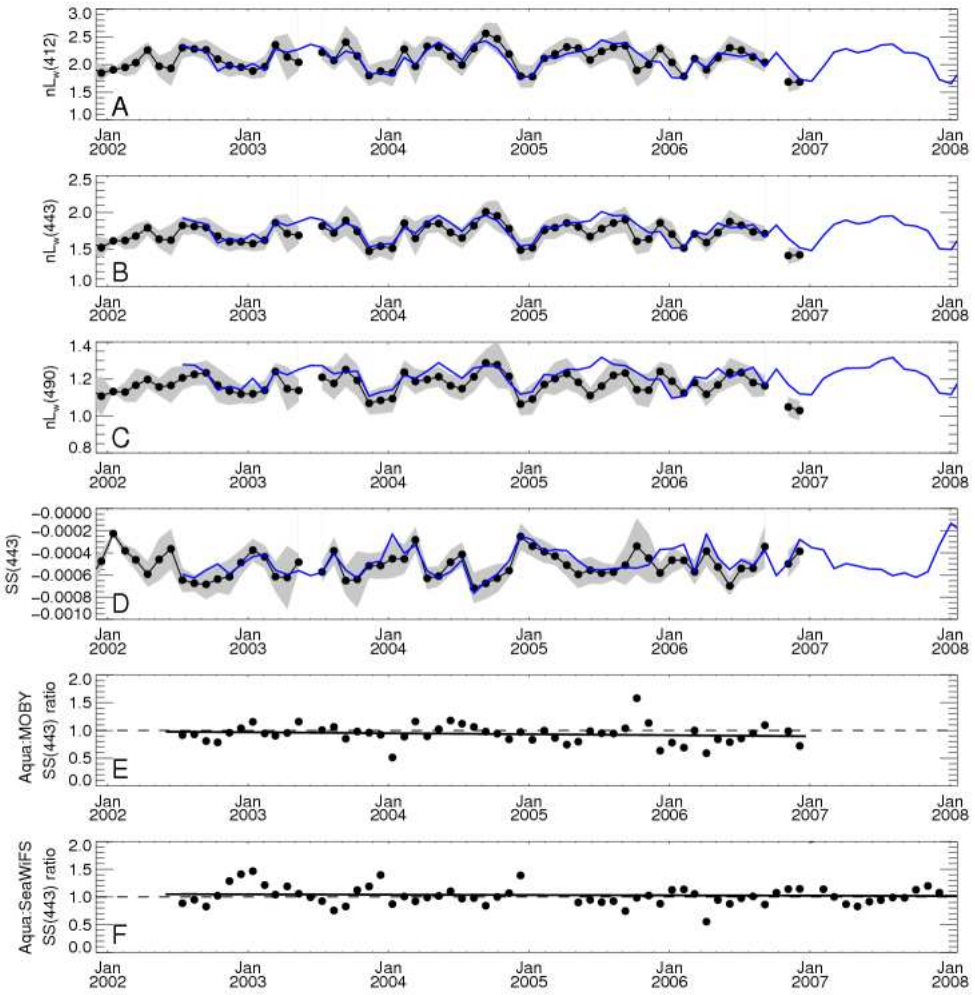


Fig. 7. Monthly time-series for Aqua (blue lines) and MOBY (black circles). Standard deviations for the MOBY monthly averages are shown in gray. The Aqua time-series was processed using a 412 nm vicarious gain adjusted by –0.25% through 2005; a standard 412-nm vicarious gain in 2006; and a 412-nm vicarious gain adjusted by + 0.25% in 2007 and 2008. Trend lines from Type I linear regression are provided in panels E and F.

### *4.4 Application*

A potential application of this approach is to tune the satellite calibration (Fig. 7). While a rigorous spectral calibration adjustment is desirable (and is the subject of subsequent work), here we simply demonstrate a mechanism for tuning the vicarious calibration using the results presented in Section 4.2. For Aqua, we applied an adjustment to the 412 band of –0.25% (adjust the standard gain by a multiplier of 0.9975) for 2002 through 2005, no adjustment of the standard gain for 2006, and an adjustment of + 0.25% (1.0025 multiplier) for 2007 and 2008. The result is a consistent shape between Aqua and both MOBY and SeaWiFS. This indicates that we can achieve an increased sensitivity of cross-calibration between satellites. Ideally, a temporally continuous (possibly linear) function of steadily increasing 412 gain would have been used for this test, rather than a step function at year-end boundaries. A mechanism to do so, however, does not currently exist in the OBPG data processing system and the development of one exceeds the scope of this preliminary case study. Despite this, the

#114396 - $15.00 USD Received 16 Jul 2009; revised 13 Nov 2009; accepted 1 Dec 2009; published 4 Jan 2010

aggregation of data into large temporal and spatial populations (e.g., annual histograms) and monthly time-series minimizes any bias introduced by our stepwise temporal gain adjustments (see, e.g., [27]).

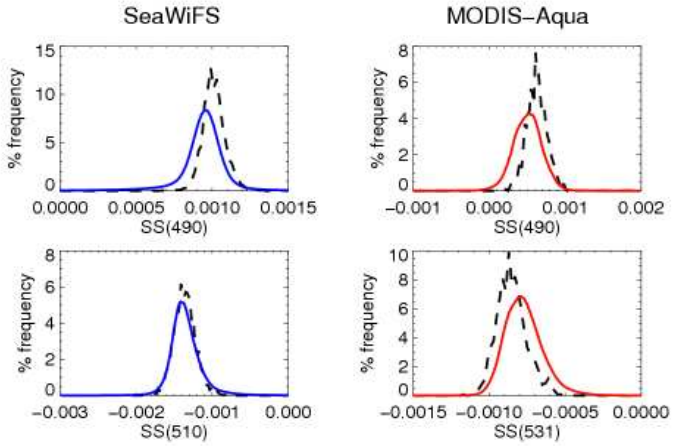


Fig. 8. Relative frequency distribution for 2003-2006 for SeaWiFS (blue lines; panels A and C) and Aqua (red lines; panels B and D) for different spectral shapes. Dashed line is MOBY distribution. Panels A and C show SeaWiFS *SS*(490) and *SS*(510) respectively. Panels B and D show Aqua *SS*(490) and *SS*(531), respectively.

Three questions arise from the analysis: (1) could it be applied to other bands; (2) could either the 443 or 490 gains be adjusted rather than the 412 gain; and, (3) could the observed drift in Aqua result from misidentification of aerosols or poor near-infrared band calibration (the spectral region used to determine the aerosols; see, e.g., [28]). Briefly, the first two questions could be considered by examining SeaWiFS *SS*(490) and *SS*(510) and Aqua *SS*(490) and *SS*(531) in greater detail (Fig. 8). These four shape histograms have well-defined, unimodal distributions. The comparisons with ground reference measurements are somewhat close, with SeaWiFS *SS*(510), in particular, having a nearly identical histogram to MOBY. SeaWiFS *SS*(555) and Aqua *SS*(551) (these bands are subsequently called 55x) are not recommended for consideration because $nL_w(670)$ is so low in clear waters that the algorithm would be driven by uncertainties in this band. The use of all the shapes would be part of a more detailed calibration.

As for the third question, it is unlikely that either changing or misidentified aerosol types or poor near-infrared band calibration directly cause the demonstrated temporal drift in Aqua. Given that the vicarious calibration and processing are consistent between SeaWiFS and Aqua, the same drift would be evident for SeaWiFS if the atmosphere near MOBY changed with time or is unrepresented in the suite of aerosol models used in the atmospheric correction process. The spectral shape of most maritime aerosols monotonically decreases with increasing wavelength [8,18,22]. Therefore, in general, any drift in $nL_w(\lambda)$ associated with selection of aerosol models, which includes the absolute temporal and spatial calibration of the near-infrared bands, would be unidirectional and most pronounced for the shortest wavelengths. The Aqua results presented in Fig. 2 suggest that the slopes of the blue bands vary in sign, with the slopes of –0.03 ( ± 0.00002), –0.006 ( ± 0.00001), and 0.003 ( ± 0.000005) μW cm$^{-2}$ nm$^{-1}$ sr$^{-1}$ year$^{-1}$, respectively, for $nL_w(412)$, $nL_w(443)$, and $nL_w(490)$.

Ultimately, a process could be established to inter-calibrate all the bands using a set of spectral shapes, which would be the most robust way to get at the decision of band correction. First, a decision would be made as to whether the blue (412 nm) or green (55x) end of the spectrum is correct. As most algorithms are based on 55x, the green end would appear to be the appropriate reference. Then, 490 is adjusted to correct the *SS*(510) or *SS*(531), followed by

#114396 - $15.00 USD Received 16 Jul 2009; revised 13 Nov 2009; accepted 1 Dec 2009; published 4 Jan 2010

443 being adjusted for *SS*(490), and finally, 412 being adjusted for *SS*(443). If the final adjustment of 412 exceeds the sensitivity limits of the standard vicarious calibration, the process could be repeated, starting with adjustment of 510 (rather than 490), until an acceptable solution is achieved.

## 5. Conclusions

Spectral shapes provide insights into how calibration can alter the spectral characteristics of the sensors. Shapes do not provide an absolute calibration, so they cannot replace any solution for absolute calibration (pre-launch and vicarious). Our shape analyses demonstrated potential for tuning the vicarious calibrations of SeaWiFS and MODIS, as well as for comparing the spectral characteristics of the sensors. In the future, such analyses could be expanded to examine other characteristics of uncertainty in the satellite data, for example, atmospheric correction for different aerosols and waters types, such as those found near the coast. Spectral shapes also provide a means of comparing various data sets, for example one sensor to another, without requiring matchup data sets. Ultimately, our analyses suggest that the annual spectral shape distribution provides a rigorous comparison of the in situ and satellite data. Future work will involve applying spectral shapes to various other in situ data sets with the goal of indentifying information that may be helpful in improving atmospheric correction of ocean color satellites, particularly in coastal waters.

## Acknowledgements

We thank members of the NASA Ocean Biology Processing Group for their valuable comments and members of the MOBY Operations Team for access to MOBY data. Funding support was provided through the NASA MODIS Science Team, the NASA Ocean Biology and Biogeochemistry Program, NRA-03-OES-02, project NNH04-AB40I, and the NOAA Integrated Program Office Project, “Assuring Ocean Color Product Consistency of NPOESS”. Initial computations were made by Kip Desch.

#114396 - $15.00 USD Received 16 Jul 2009; revised 13 Nov 2009; accepted 1 Dec 2009; published 4 Jan 2010